ESKİŞEHİR TECHNICAL UNIVERSITY JOURNAL OF SCIENCE AND TECHNOLOGY
A- APPLIED SCIENCES AND ENGINEERING

2023, 24(3), pp. 164-176, DOI:10.18038/estubtda.1197024

RESEARCH ARTICLE

ENHANCEMENT OF HEAT TRANSFER WITH VISCOUS DISSIPATION IMPACT ON FLUID FLOW PAST A MOVING WEDGE IN A PERMEABLE DOMAIN

Uchenna Awucha UKA [1], Innocent Chukwuemeka EMEZIEM [2], Semiu Akinpelu AYINDE [3]

Charles ADENIKA [3], Kelvin Onyekwere AGBO [3]

[1, 3] Department of Basic Sciences, School of Science and Technology, Babcock University, Ogun State, 121003, Nigeria

[2]Department of Mathematics, College of Physical and Applied Sciences, Michael Okpara University of Agriculture, Umudike, Abia State, 440101, Nigeria

ABSTRACT

The problem of modelling and analysis of fluid flow in the presence of viscous dissipation as a result of a wedge in motion is analytically and numerically deliberated upon. The much-valued significance of this study in the aspects of technological and industrial revolution include aerospace, oil recovery systems, defence machineries, extrusion, moulding and polymerisation of sheets, building of war arsenal and glass whirling. However, the frontiers of several physical problems are modelled by both partial and ordinary differential equations (PDEs and ODEs). Therefore, the mathematical modelling of our present problem is not an exemption. Hence, the PDEs in which our problem under consideration is modelled become reformed into coupled ODEs in nonlinear form through the deployment of adequate and standard conversion procedure with dimensionless variables. In line with the approach of our solution methodology, the boundary conditions governing the flow models are also transmuted. Afterwards, the well-established regular perturbation skill aided in the resolution of the problem. The solutions realized are simulated through the adoption of a software package (Mathematica V.10 scheme) for the numerical solutions. Our numerical results are embodied in form of graphs and legends. It is worthy to note that an increase in the rate of flow remains a function of effect of rising values of the porosity and Grashof thermal parameters whereas the opposite behaviour of the flow field is linked to improving values of suction parameter. Also, the enhancement of the suction parameter and Eckert number breeds intensification in the temperature. Similarly, an enhancement in the values of Prandtl number, $Pr = 0.7,\ 1.5,\ 5.0,\ 7.0$ with radiation parameter, $A = 0.1$, and Eckert number $Ec = 0.2$ showed an increase in the rate of heat transfer i.e., $-\varphi'(0) = 0.7594,\ 1.9077,\ 10.5114,\ 17.9537$. Hence, the Nusselt number intensifies with the rising values of the Prandtl parameter.

Keywords: Heat transference, Porous medium, Perturbation, Simulation, Viscosity

1. INTRODUCTION

The study of fluid viscosity forms an important part of thermal augmentation in its application to heat exchangers machinery. The fluid viscidness helps in transferring and transforming thermal energy across the flowing fluid and this process impacts hotness to the fluid. Hence, this partly irretrievable procedure is termed viscous dissipation. Thus, the shear strain plays a vital role in the transformation, thermally. The significance of this research is valued in the area of scheming chilling devices, thermal loss of different forms in improving thermal conductivity characteristics of an isothermal flow leading to a surge in their technological advancement and applications. Meanwhile, in the study of fluid flows over a wedge, informs a typical issue in the general behavioural pattern of dynamical fluid system. Therefore, applications of wedge flow ranges from mechanical, petrochemical, geological engineering and technology etc. Hence, the progress made in controlling and enhancing the rate of thermal conductivity in various engineering, technological, production, metallurgical and packaging firms cannot be overemphasised. The initial investigation of incompressible fluid viscosity past a wedge using the Falkner-Skan equation remains the concept of [1]. The analytical simulation of this equation using

*Corresponding Author: ukau@babcock.edu.ng
Received: 31.10.2022 Published: 22.09.2023

numerical dwindling velocity distribution was studied by [2]. Lately, several researchers developed keen interest in studying transmission of fluid over a wedge material. Thus, the deployment of Dirichlet with Robin heat conditions at the boundary was studied by [3, 4, 5]. Later on, Shit and Majee [6] examined the influence of heat radiation and chemical reaction on MHD fluid passage over a dual disposed elastic plate with non-constant viscosity due to thermal source/sink. They inferred that radiation as well as heat source/sink determines to a large extent, the rate at which heat is conveyed at wall section. The numerical analysis involving hydromagnetic slip movement of liquid filled with nanofluid over a wedge in the presence of convectively thermal source/drip was shared by [7].

The application of chemical reactions in the presence of fluid flow has proved very useful in diverse industrial uses, such as in food handling firms and paint production companies, etc. Hence, Sulochana et al. [8] through analytical means studied free and forced convection Casson nanofluid past a diagonal material. They maintained that improved concentration of fluid and transmission mass ratio is achieved because of appreciating values of chemical reactivity. The MHD Falkner-Skan wall layer passage with interior energy supply/drop was discussed by [9]. Their result established a difference in heat supply/lag on transmission speed of thermal energy when compared to its rate on the skin-friction coefficient. Few years ago, some research on nanofluid flow over a wedge has been carried out by [10, 11, 12 and 13]. The report on non-Newtonian equation over a nonlinearly elongating plate with different external factors was achieved by [14]. However, Aman et al. [15] inspected a nanofluid flow with small-particles in form of gold due to the impact of radiation as well as transverse diffusion on the distribution field. A fluid prototype surrounded by Riga sheets with an architype flow having stretching and viscosity features amid a sloping conduit has been established by [16, 17]. In recent times, Ullah et al. [18] explored the inspiration of enforced Lorentz effects on a non-Newtonian flow. Similarly, flow over a wall layered nanofluid past a moving wedge was presented by [19]. An examination on the flow and thermal transportation characteristics in a viscous fluid past a nonlinearly stretched plate was conducted by Vajravelu [20]. The fourth-order Runge–Kutta integration approach was used in the solution of his problem. It was found that the heat flow moves from the stretching plate towards the fluid. The influence of Hall current and heat radiation on thermal and mass transportation of a chemically reacting MHD flow of a micropolar fluid over a permeable sheet was studied by Oahimire and Olajuwon [21]. They applied perturbation scheme in order to solve the dimensionless equations. Their results indicated that a rise in the strength of magnetic field leads to a fall in the fluid motion in the direction of the sheet. Recently, hydromagnetic stream and thermal problems have received important motivation at a high level. Thus, the analysis of the effect of hall current, chemical reaction and radiation on a natural convective flow confined by a vertical medium immersed in a spongy surface due to the influence of unvarying magnetic field was scrutinized by Tavva et al. [22]. They applied the simple perturbation method in solving the problem. Their findings showed that both velocity and concentration surges as a result of multiplicative reactions and declines due to a destructive reaction.

Similarly, Kumar et al. [23] considered the impact of Hall current, radiation, Soret as well as Dufour numbers on an unsteady MHD free convection flow through an infinite vertical stationary sheet in an absorbent media. The solution of the dimensionless equations with the boundary constraints were made possible by utilizing the Galerkin technique. It was observed that as the Soret factor enhances, the concentration distribution improves and opposite movement was noticed in terms of Dufour parameter. Accordingly, Cortell [24] performed a numerical examination in line with the boundary layer flow prompted in a quiescent fluid due to continuous plate stretching as a result of the velocity $u_w = (x) \sim x^{\frac{1}{3}}$ in the presence of thermal transfer. The Runge-Kutta fourth order scheme and shooting method were used in solving the problem. From the result, the temperature rises as the temperature ratio number increase and it depreciates as thermal radiation factor improves. The investigative analysis of heat and mass distribution impact on the flow past a stretching sheet with thermal source was investigated by Barik et al. [25]. The solution was carried out by applying Kummer's function. It was noted that tougher suction bound with magnetic field interaction led to a decline in the skin friction coefficient.

In the course of reviewing the above literatures, it's obvious that there's a short fall in analysing the impartation of viscosity degeneracy, absorbent medium and suction numerically on a fluid flow over a non-static wedge. Therefore, we shall take the afore-mentioned flow characteristics into account in this present study. Meanwhile, this work is organised into 5 parts starting with the introduction which contains the significance of the current analysis and review of other studies as the first part. In part 2, the mathematical models of the problem under consideration and the flow arrangement was formulated and presented while part 3 consists of the methodology applied in the solution process and part 4 depicts the gained results and their discussion, followed by the conclusion.

2. FORMULATION OF PROBLEM AND BASIC MODELS

An incompressible, steady laminar hydrodynamic conducting fluid movement over a wedge is appropriated. The coordinated systems due to the $x-axis$ corresponding to the wedge wall is positioned while the normal is along $y-axis$, with constant pressure, p. However, there's an indented angle in tune with the wedge external surface as depicted in figure 1, where
$\alpha = wedge\, angle$. The wall and neighbourhood temperatures of the wedge refers to T_s and T_∞. respectively.

Hence, the following deductions ensue:

- An electrically conducting steady fluid stream equation is provided.
- Impression of degeneracy, porosity with radiative energy is reasoned.
- A constant pressure, p is considered.

In the light of the Boussineq estimate and conditions, the mathematical models of the flow emerges: 2.1

Continuity Equation

$$\frac{\partial u'}{\partial x'} + \frac{\partial v'}{\partial y'} = 0 \tag{1}$$

2.2 Momentum equation

$$u'\frac{\partial u'}{\partial x'} + v'\frac{\partial v'}{\partial y'} = \vartheta\frac{\partial^2 v'}{\partial y'^2} + \frac{v}{k'}u' - \frac{1}{\rho}\frac{\partial p'}{\partial x'} + g\alpha_T(T' - T'_\infty)l^2 \tag{2}$$

2.3 Energy conservation equation

$$u'\frac{\partial T'}{\partial x'} + v'\frac{\partial T'}{\partial y'} = \frac{\mu}{\rho c_p}\frac{\partial^2 T'}{\partial y'^2} + \frac{\mu}{\rho c_p}(T' - T'_\infty) - \frac{k'}{\rho c_p}\frac{\partial qr}{\partial y'} \tag{3}$$

With wall restrictions stated as

$$\left.\begin{aligned} &u = U_w = bx^n,\ v = -m,\ T' = T'_s,\ C' = C'_s && \text{at } y = 0 \\ &u \to 0,\ \ T' \to T'_\infty,\ \ C' \to C'_\infty && \text{as } y \to \infty \end{aligned}\right\} \tag{4}$$

The similarity transformation characteristics include:

$$\eta = y\sqrt{\frac{b(n+1)}{2v}}x^{\frac{(n-1)}{2}}, \quad u = bx^n f'(\eta),\ T' - T'_\infty = (T'_s - T'_\infty)\theta(\eta) \tag{5}$$

$$v = -\sqrt{\frac{bv(n+1)}{2}}\ x^{\frac{n-1}{2}}\left[f(\eta) + \left(\frac{n-1}{n+1}\right)\eta f'(\eta)\right] \tag{6}$$

Where,
$e_0 > 0$ and $e_0 < 0$ are suggestive of suction and injection accordingly. Meanwhile, equation (1) stands for the non-compressible steady continuity equation and equation (2) defines the fluid momentum equation. Equation (3) establishes that heat drift in the fluid takes place in view of convection, reaction

of viscous dissipation and radiative flux, as represented by the first, second and third terms respectively on the right-hand side.

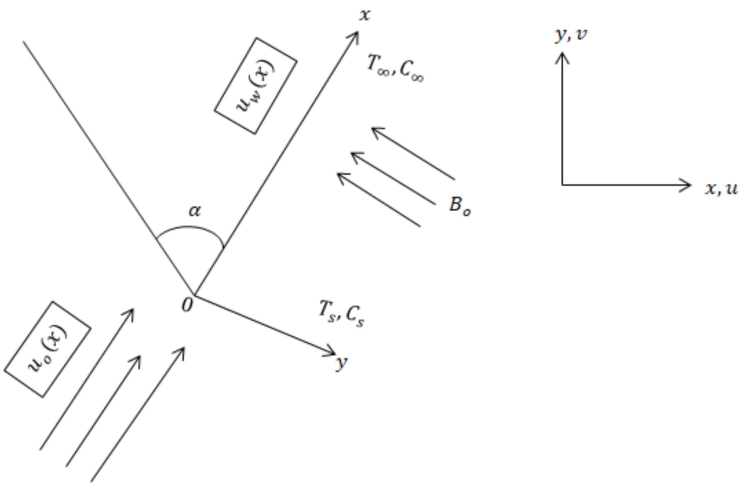

Figure 1. Physical representation of wedge flow

From the relation above, we have l, g as characteristics length and acceleration regarding gravity. Also, the following terms $\vartheta, \rho, C_p, q_r, k, \sigma, p, T, x$ and y are dynamic velocity, density, capacity of heat, thermal radiative flux, permeability constant, electrical conductivity, pressure, fluid temperature, direction of axes of the velocity components with $u = \frac{\partial \psi}{\partial y}$, $v = -\frac{\partial \psi}{\partial x}$.

3. SOLUTION APPROACH

By adopting the approximation of Rosseland equalities [27] in case of radiation, with

$$q = -\left(\frac{4\sigma^*}{3m_*}\right)\frac{\partial T'^4}{\partial y} \quad (7)$$

With

$\sigma^* \approx 1.3806 \times 10^{-23}$ as Stefan-constant term, $m_* =$ average absorption quantity. Taking the expansion of T^4 about T_∞ in terms of Taylor's series gives

$$T^4 = T_\infty^4 + 3T_\infty^3(T - T_\infty) + 6T_\infty^2(T - T_\infty)^2 + \cdots \quad (7a)$$

Ignoring terms in greater index produces

$$T^4 \cong 4TT_\infty^3 - 3T_\infty^4 \quad (8)$$

Noting that

$$\frac{\partial p'}{\partial x'} = 0 \quad (9)$$

Similarly, using equations (7) – (8) into equation (3) simplifies to

$$u'\frac{\partial T'}{\partial x'} + v'\frac{\partial T'}{\partial y'} = \frac{\mu}{\rho c_p}\frac{\partial^2 T'}{\partial y'^2} + \frac{\partial^2 T'}{\partial y'^2}\frac{16\sigma^* T_\infty^3}{3m_f^*} + \frac{\mu}{\rho c_p}(T' - T'_\infty) \quad (10)$$

Transformation of equations (2), (4) and (10) with the non-dimensional variables in equations (5) and (6) assumes

$$\frac{d^3f}{d\eta^3} + f(\eta)\frac{d^2f}{d\eta^2} + Kr\frac{df}{d\eta} + Gl\theta(\eta) = 0 \quad (11)$$

$$\frac{d^2\theta}{d\eta^2}(1 + A) + Prf(\eta)\frac{d\theta}{d\eta} + PrEc\theta(\eta) = 0 \quad (12)$$

$$\frac{df}{d\eta} = 1,\ f(\eta) = m_o, \theta(\eta) = 1 \qquad \text{at } \eta = 0 \quad (13)$$

$$\frac{df}{d\eta} \to 0, \qquad \theta(\eta) \to 0 \qquad \text{as } \eta \to \infty \quad (14)$$

Where,

$K = \frac{k' v_o^2}{v^2}$, $A = \frac{16\sigma^* T_\infty^3}{3k^* k}$, $Pr = \frac{\mu C_p}{k}$, $Ec = \frac{u^2}{C_p \Delta T} \ni \Delta T = T_s' - T_\infty'$, $Gl = \frac{\alpha_T l^2 g(T_s - T_\infty)}{uv}$, specify the Porosity, radiation, Prandtl, Eckert and local thermal Grashof relations.

3.1. Analytical Solution

The analytical solution of the problem has been carried out by utilizing the regular perturbation method. It is a mathematical technique used to obtaining approximate solutions for differential equations that contain a small parameter, say Γ. This technique is mainly useful when the differential equation is coupled, difficult or impossible to be solved directly but can be simplified by assuming that the small parameter Γ is much smaller than 1.

Step 1: We need to state or write down an ordinary differential equation involving a small parameter Γ.
Step 2: We assumed that the solution can be expressed as a power series in terms of the small parameter Γ: i.e., $y(\eta) = y_0(\eta) + \Gamma y_1(\eta) + \Gamma^2 y_2(\eta) + \cdots$ (15)
where $y_0(\eta), y_1(\eta), y_2(\eta)$, etc., are functions that are to be determined.
Step 3: We substituted the assumed solution into the original ODE in order to obtain a series of equations.
Step 4: We equated coefficients of different powers of Γ, so as to generate a set of equations involving the unknown functions $y_0(\eta), y_1(\eta), y_2(\eta)$, etc. These equations were solved to determine the expressions for the unknown functions.
Step 5: As soon as the expressions for $y_0(\eta), y_1(\eta), y_2(\eta)$, etc., were found, we substituted them into the assumed solution of equation (15) to realize the approximate solution, $y(\eta)$.
Step 6: We applied the boundary conditions (given) to determining the integration constants that appeared in the solutions obtained in Step 4 above.

Relating to Bestman [28], we have

$$\eta = \Delta e_0, \quad f(\eta) = e_0 F(\eta), \quad \theta(\eta) = \varphi(\eta), \quad \Gamma = \frac{1}{{e_0}^2} \quad (16)$$

Inputting equation (16) and its differentials into equations (11) – (12) produces,

$$\frac{d^3f}{d\eta^3} + f(\eta)\frac{d^2f}{d\eta^2} + \Gamma K\frac{df}{d\eta} + \Gamma^2 Gl\varphi(\eta) = 0 \quad (17)$$

$$\frac{d^2\varphi}{d\eta^2}(1 + A) + Prf(\eta)\frac{d\varphi}{d\eta} + \Gamma\varphi(\eta)PrEc = 0 \quad (18)$$

Which depends on:

$$\left.\begin{aligned} &\eta = 0; \quad f = 1,\ \frac{df}{d\eta} = e_0,\ \varphi = 1 \\ &\eta \to \infty; \quad \frac{df}{d\eta} \to 0, \qquad h \to 0 \end{aligned}\right\} \quad (19)$$

The application of the regular perturbation technique in resolving equations (17) and (18) follows. Thus, let the series solution be:

$$f(\eta) = 1 + \sum_{k=n=1}^{\infty} (\Gamma)^k f_n(\eta) \tag{20}$$

$$\varphi(\eta) = \sum_{k=n=1}^{\infty} (\Gamma)^k \varphi_n(\eta) \tag{21}$$

Differentiating equations (20) trice and (21) twice in terms of η, using the results in equations (17) – (18) and simplifying, shows that at zeroth order, we have:

$$\frac{d^2\varphi_o}{d\eta^2}(1 + A\ ) + Pr\frac{d\varphi_o}{d\eta} = 0\text{: } \varphi_o(0) = 1, \varphi_o(\infty) = 0 \tag{22}$$

Evaluating at order one (1) provides:

$$\frac{d^3 f_1}{d\eta^3} + \frac{d^3 1}{d\eta^3} = 0\text{: } f_1(0) = 0, f_1{}'(0) = 1,\ \ f_1{}'(\infty) = 0 \tag{23}$$

$$\frac{d^2\varphi_1}{d\eta^2}(1 + A) + Pr\frac{d\varphi_1}{d\eta} + Prf_1(\eta)\frac{d\varphi_o}{d\eta} + EcPr\varphi_o(\eta) = 0\text{: } \varphi_1(0) = 0, \varphi_1(\infty) = 0 \tag{24}$$

In terms of order two (2), we gained

$$\frac{d^3 f_2}{d\eta^3} + \frac{d^3 f_2}{d\eta^3} + f_1(\eta)\frac{d^2 f_1}{d\eta^2} + K\frac{df_1}{d\eta} + Gl\varphi_o(\eta) = 0\text{: } f_2(0) = 0, f_2{}'(0) = 0, f_2{}'(\infty) = 0 \tag{25}$$

The analytical solutions mentioned below are obtained by solving equations (22) – (25) in line with their appropriate and respective wall conditions.

$$f'(\eta) = exp - \eta + \frac{1}{(e_o)^2}\Big(-\eta exp - \eta - exp - \eta - \frac{1}{2}exp - 2\eta + k\eta exp - \eta + kexp - \eta - \frac{Gl}{j(j-1)}exp - j\eta + S_4 - S_6 exp - \eta\Big) \tag{26}$$

$$\varphi(\eta) = exp - j\eta + \frac{1}{(e_o)^2}\Big(-j\eta exp - j\eta - \frac{(j)^2}{1+j}exp - (1+j)\eta + Ec\eta exp - j\eta + \frac{(j)^2}{1+j}exp - j\eta\Big) \tag{27}$$

With,

$S_4 = 0, S_6 = k - \frac{3}{2} - \frac{Gl}{j(j-1)}, j = \frac{Pr}{1+A}$ as the constants.

Nonetheless, in the engineering designing of various forms of devices, the Nusselt number, Nu which represents the rate at which thermal energy is conveyed through a given scheme, becomes very relevant. Thus,

$$Nu = \varphi'(\eta) = -(1 + A)\left(\frac{\partial\varphi}{\partial\eta}\right)_{\eta=0} \tag{28}$$

3.2. Numerical Simulation

The Mathematica scheme and Wolfram language have been applied to finding the numerical results of equations (26) – (28) respectively. Hence, such solutions are offered in form of graphs containing legends as demonstrated below.

4. RESULTS AND DISCUSSION

From the graphical results, $f'(\eta)$ and $\varphi(\eta)$ implies velocity and temperature of flowing fluid and represents the vertical axis while the independent variable, η is on the horizontal axis.

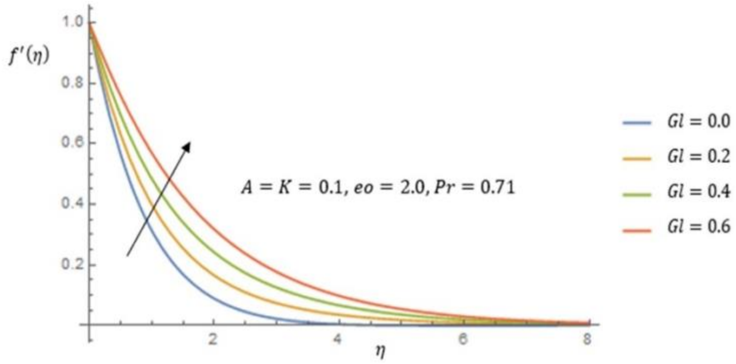

Figure 2. Influence of local thermal Grashof parameter, Gl on the fluid flow rate

In Figure 2, as the dominance of the buoyancy force proportion overshadows the viscous force, the flow field rises. Thus, the flow rate $f'(\eta)$, heightens as the dimensionless fluid parameter values of Gl increases. The result of varying the values of radiation A in ascending array, on the momentum and temperature of the moving fluid is visualized in Figures 3 and 4, accordingly. However, the introduction of this parameter (A) into the flow, changes heat energy into kinetic form and as it augments continually, both $f'(\eta)$ and $\varphi(\eta)$ intensifies.

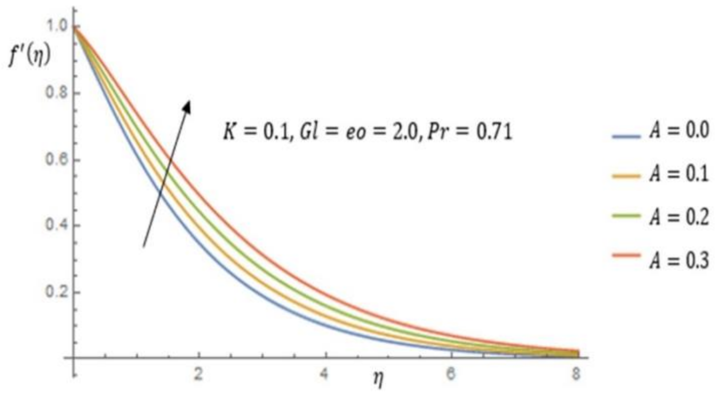

Figure 3. Influence of radiation constraint, A on the fluid flow rate

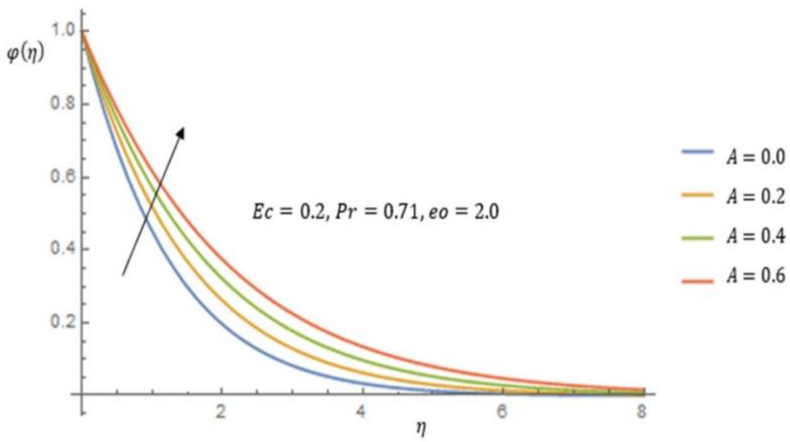

Figure 4. Influence of radiation number, A on the energy transmission rate

The impact of the permeability factor, k is explained in Figure 5. Meanwhile, due to the spongy nature of the medium through which the fluid flow takes place, the rate of tide changes dynamically resulting to a surge in momentum boundary layer. Thus, the upsurge in the values of k, leads to an appreciable enhancement in the flow distribution of $f'(\eta)$.

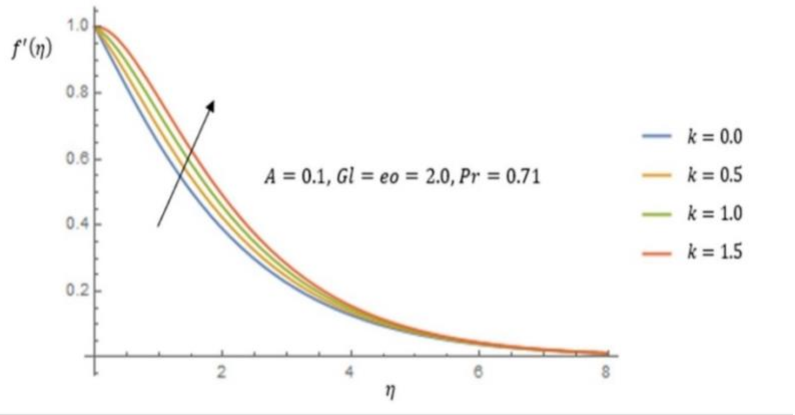

Figure 5. Influence of porosity constraint, k on the fluid flow rate

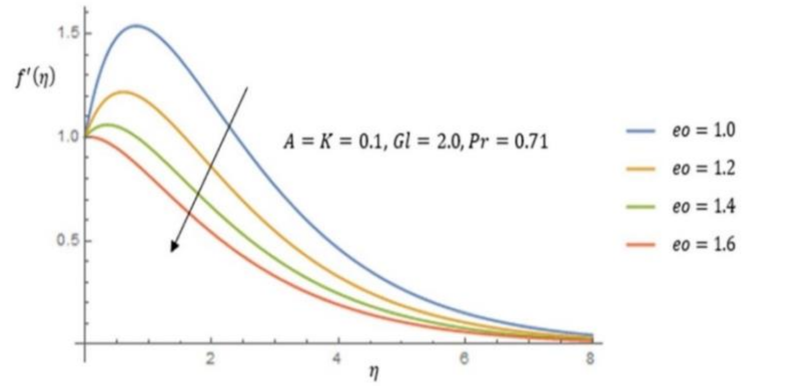

Figure 6. Influence of suction constraint, e_o on the fluid flow rate

Similarly, the development of $f'(\eta)$ and $\varphi(\eta)$ owing to the effects of suction parameter, eo on fluid rate and thermal transfer are depicted in Figures 6 and 7 respectively. Whence, raising the values of this parameter informs increasing speed of fluid motion, $f'(\eta)$ and thermal boundary layer with a rising field of $\varphi(\eta)$.

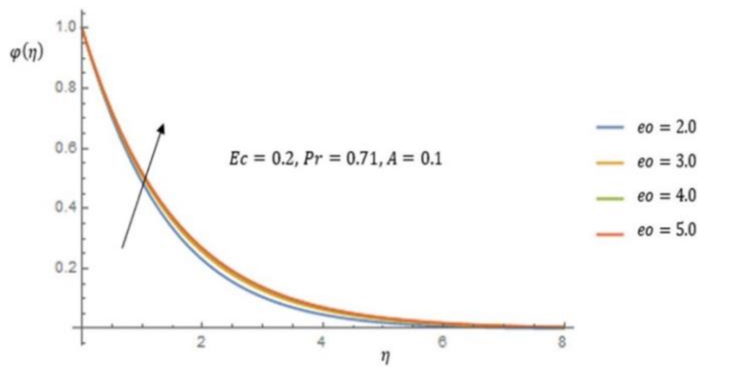

Figure 7. Influence of suction number, e_o on the energy transmission rate

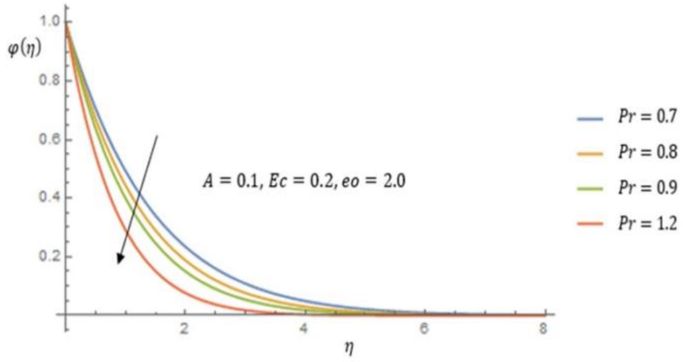

Figure 8. Influence of Prandtl factor, Pr on the energy transmission rate

Figure 8, captures the result of the uprising effect of Pr on temperature. Meanwhile, the ratio of viscous to thermal diffusivity rate is referred to as Prandtl factor. Therefore, as a non-dimensional number, when $Pr \ll 1$, the thermal boundary layer thickness becomes bigger when compared with $Pr \gg 1$. Therefore, improving the values of Pr reflects a fall in $\varphi(\eta)$.

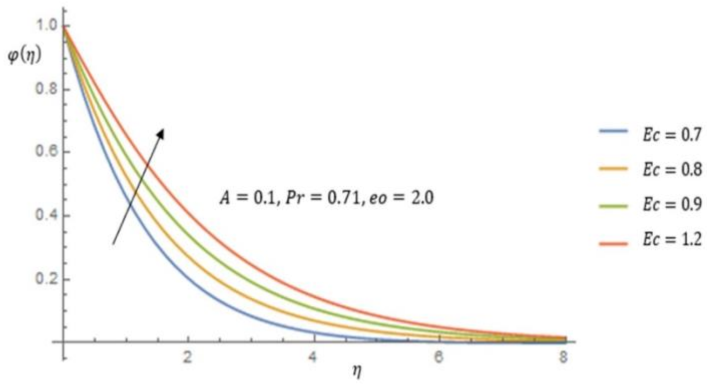

Figure 9. Influence of Eckert constraint, Ec on the energy transmission rate

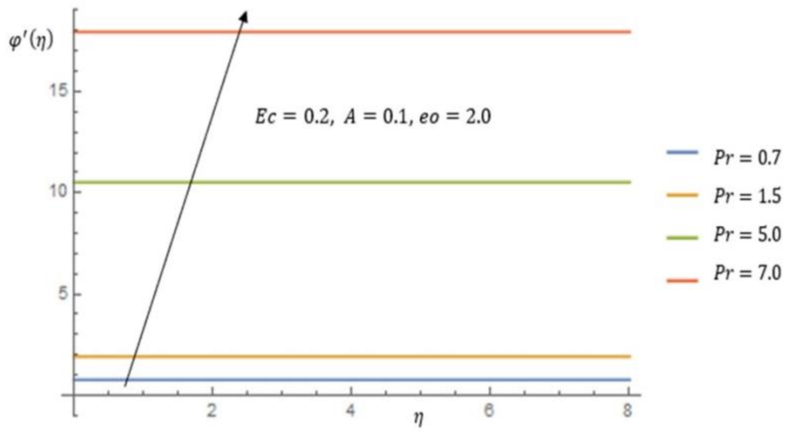

Figure 10. Influence of Pr on Nusselt number, Nu

In Figure 9, the influence of Eckert constraint, Ec on $\varphi(\eta)$ of fluid stream is obvious. The dimensionless number, Ec relates to the connection concerning the flow's energy kinetically with energy variance existing at the wall in terms of debauchery through heat transference. Thus, appreciating values of Ec embraces increment in the fluid's temperature, $\varphi(\eta)$. The stimulus as a result of enhancing values of Pr

on Nu, is referenced in Figure 10. When $Pr < 1$, heat spreads slowly but at $Pr > 1$, the rate of thermal transference intensifies as shown in Table 1 below and the above mentioned Figure 10. Thus, growing values of Pr aids in regulating the speed at which a conducting fluid cools in a given system. Therefore, heat disperses quickly thereby helping to guide the temperature of a given device functioning with the dynamics of fluid flow in several physical applications. However, the evolving changes on thermal transmission rate, (Nu) as a result of increasing values of A are highlighted in both Table 2 and Figure 11. Nevertheless, from these two forms of data presentations, it can be detected that as A improves, the rate of heat conveyance, (Nu) recedes.

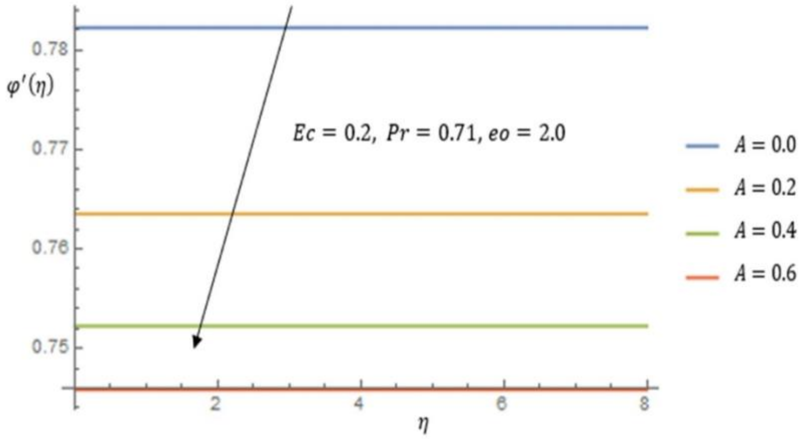

Figure 11. Influence of A, on Nusselt number, Nu

Table 1. Nusselt number coefficient for varying values of Pr at $e_o = 2.0$

A	Ec	Pr	$-\varphi'(0)$
0.1	0.2	0.7	0.7594
0.1	0.2	1.5	1.9077
0.1	0.2	5.0	10.5114
0.1	0.2	7.0	17.9537

Table 2. Nusselt number coefficient for varying values of A at $e_o = 2.0$

A	Ec	Pr	$-\varphi'(0)$
0.0	0.2	0.71	0.7822
0.2	0.2	0.71	0.7635
0.4	0.2	0.71	0.7523
0.6	0.2	0.71	0.7458

5. CONCLUSION

The analysis of the influence of viscous degeneracy for the augmentation of thermal transferal over a moving wedge in a porous domain is deliberated. From the results obtained by means of using perturbation approach and an in-built Wolfram Mathematica solver, the following concluding remarks are made.

(a) The momentum boundary layer increases as Gl and k improves in their values, thus leading to upsurge in the fluid velocity.

(b) There is an increase in the fluid's velocity, $f'(\eta)$ and temperature, $\varphi(\eta)$ as the values of radiation A and suction eo parameters enhances.

(c) Increasing values of Ec raises the thermal wall layer such that $\varphi(\eta)$ of the fluid grows while the reverse is the condition when Pr improves.

(d) The rate of heat transfer, Nu is brought under control through cooling when Pr intensifies whereas for A, the opposite is the outcome.

Meanwhile, in line with the current study, the suggestive areas of future research include numerical simulations and optimization techniques: Thus, the conduction of advanced numerical simulations using Computational Fluid Dynamics (CFD) and optimization procedures to study the fluid flow and heat transfer characteristics over a moving wedge in a porous chamber due to viscous dissipation remains a future research area to be explored. Also, the investigation of diverse geometries, permeability distributions, and wedge motion patterns to optimize the heat transfer performance and identify the most efficient configuration, forms another area of future research.

CONFLICT OF INTEREST

We state that there are no conflicts of interest of any type as regards to the publication of this article.

ACKNOWLEDGEMENT

We wish to appreciate the referees for their constructive input towards the improvement of this study.

AUTHORSHIP CONTRIBUTIONS

Conceiving and designing of the research study by Uchenna Awucha Uka[1]; Contributions to the theoretical framework of the research through the provision of critical intellectual input throughout the research process by Uchenna Awucha Uka[1], Innocent Chukwuemeka Emeziem[2], Semiu Akinpelu Ayinde[3], Charles Adenika[3], Kelvin Onyekwere Agbo[3]; Solution of the transformed mathematical model by Uchenna Awucha Uka[1], Innocent Chukwuemeka Emeziem[2] and Charles Adenika[3]; Contributions on result analysis, interpretation of results, participation in the revision and formatting of the research manuscript by Uchenna Awucha Uka[1], Innocent Chukwuemeka Emeziem[2], Semiu Akinpelu Ayinde[3], Charles Adenika[3], Kelvin Onyekwere Agbo[3]; Provision of subject matter expertise, reviewed and revised the manuscript for clarity and scientific rigor and ensured adherence to ethical considerations by Uchenna Awucha Uka[1] and Innocent Chukwuemeka Emeziem[2]; Re-checking of the article not only for spelling and grammar but also for intellectual content before submission by Uchenna Awucha Uka[1], Innocent Chukwuemeka Emeziem[2], Semiu Akinpelu Ayinde[3], Charles Adenika[3], Kelvin Onyekwere Agbo[3].

Supervision of the overall research project and provision of guidance throughout the research process by Uchenna Awucha Uka[1]; Also, all the authors played a significant role in the manuscript revision and its final approval.

Therefore, all the authors have read and approved the final version of the manuscript and have agreed to its submission for publication.

REFERENCES

[1] Falkner VM, Skan SW. Solutions of the boundary layer equations. Philosophical Magazine 1931; 7: 865-896.

[2] Fang T, Yao S, Zhang J, Zhang Y, Tao H. Momentum and heat transfer of the Falkner-Skan flow with algebraic decay: an analytical solution. Commun. Nonlinear Sci. Numer Simul 2012; 17(6): 2476-2488.

[3] Ashraf M, Narahari M, Muthuvalu MS. Mixed convection flow over a stretching porous wedge with Newtonian heating in the presence of heat generation or absorption. In: AIP Conference Proceedings 2016; 1787, 020004, AIP, New York.

[4] Ahmad K, Hanouf Z, Ishak A. MHD Casson nanofluid flow over a wedge with Newtonian heating. Eur. Phys. J. Plus 2017; 132(2): 87.

[5] Hossain M, A Roy NC, Siddiqa S. Unsteady mixed convection dusty fluid flow over a vertical wedge with small fluctuation in free stream and surface temperature. Appl. Math. Comput 2017; 293: 480-492.

[6] Shit GC, Majee S. Hydromagnetic flow past an inclined nonlinear spreading material with fickle viscosity in the presence of thermal radiation and chemical reaction. Journal of Applied Fluid Mechanics 2014; 7(2): 239-247.

[7] Rahman MM, Al-Lawatia MA, Eltayeb AI, Al-Salti N. Hydromagnetic slip flow of water based nanofluids past a wedge with convective surface in the presence of heat generation/absorption. International Journal of Thermal Sciences 2012; 57: 172-182.

[8] Sulochana G, Ashwinkumar GP, Sandeep N. Effect of frictional heating on mixed convection flow of chemically reacting radiative Casson nanofluid past an inclined porous plate. Alex. Eng J 2018; 57(4): 2573-2584. https://doi.org/10.1016/j.aej.

[9] Ashwini G, Eswara AT. MHD Falkner-Skan boundary layer flow with internal heat generation or absorption . World Academy of Science, Engineering and Technology 2012; 65: 662-665.

[10] Khan WA, Pop I. Boundary layer flow over a wedge passing in a nanofluid. Mathematical Problems in Engineering 2013; 637-285.

[11] Yacob NA, Ishak A, Nazar R, Pop I. Falkner-Skan problem for a static and moving wedge with prescribed surface heat flux in a nanofluid. International Communications in Heat and Mass Transfer 2011; 38: 149-153.

[12] Chamkha AJ, Abbasbandy S, Rashad AM, and Vajravelu K. Radiation effects on mixed convection over a wedge immersed in a permeable medium filled with a nanofluid. Transport in Porous Media 2012; 91: 261-279.

[13] Kasmani RM, Muhaimin I, Kandasamy R. Laminar boundary layer flow of a nanofluid along a wedge in the presence of suction/injection. Journal of Applied Mechanics and Technical Physics 2013; 54(3): 377-384.

[14] Ullah I, Bhattacharyya K, Shafie S, Khan I. Unsteady MHD mixed convection slip flow of Casson fluid past nonlinearly stretching sheet embedded in a porous medium with chemical reaction,

thermal radiation, heat generation/absorption and convective boundary conditions. Public Library of Science One (PLoS ONE) 2016; 10(11) http://doi.org/10.1371/journal.pone.0165348.

[15] Aman S, Khan I, Ismail Z, Salleh MZ. Impacts of gold nanoparticles on MHD mixed convection Poiseuille flow of nanofluid passing through a porous medium in the presence of thermal radiation, thermal diffusion and chemical reaction. Naural Computing and Applications 2016; 30(3): 14 789-797.

[16] Ahmed N, Khan U, Mohyud ST. Influence of an effective Prandtl number model on squeezed flow of $\gamma AL2O3 - H2O$ and $\gamma AL2O3 - C2H6O2$ nanofluids. Journal of Molecular Liquids 2017; 238: 447- 17 454.

[17] Adnan M, Asadullah M, Khan U, Ahmed N, Mohyud-Din ST. Analytical and Numerical investigation of thermal radiation effects on flow of viscous incompressible fluid with stretchable convergent/divergent channels, Journal of Molecular Liquid 2016; 224: 768-775.

[18] Ullah K, Bhattacharyya K, Shafie S. Hydromagnetic Falkner-Skan flow of Casson fluid over a moving wedge due to heat transfer. Alexandria Engineering Journal 2016; 55(3): 2139-2148.

[19] Khan AW, Pop I. Math. Prob. Eng 2013; 1-7.

[20] Vajravelu K. Viscous flow over a nonlinearly stretching plate. Applied Mathematics and Computation 2001; 124(3): 281-288.

[21] Oahimire, JI, Olajuwon BI. Effect of Hall current and thermal radiation on heat and mass transfer of a chemically reacting MHD flow of a micropolar fluid past a porous medium. Journal of King Saud University-Engineering Sciences 2013; 1-10. http://dx.doi.org/10.1016/j.jksues.2013.06.008.

[22] Tavva SR, Reddy OSP, Raju MC, Varma SVK. MHD free convection heat and mass transfer flow through a porous medium bounded by a vertical surface in the presence of hall current. Advances in Applied Science Research 2012; 3(6): 3482-3490.

[23] Kumar MA, Reddy YD, Goud BS, Rao VS. Effects of Soret, Dufour, Hall current and radiation on MHD natural convective heat and mass transfer flow past an accelerated vertical plate through a porous medium. International Journal of Thermofluids 2021; 9: 100061. https://doi.org/10.1016/j.ijft.2010100061.

[24] Cortell R. Fluid flow and radiative nonlinear heat transfer over a stretching sheet. Journal of King Saud University-Engineering Sciences 2014; 26: 161-167. https://dx.doi.org/10.1016/j.jksus.2013.08.004.

[25] Barik RN, Dash GC, Rath PK. Heat and mass transfer on MHD flow through a porous medium over a stretching surface with heat source. Mathematical Theory and Modeling 2012; 2(7): 49-59.

[26] Boussinesq J. Analytical Theory of Heat. Gauthier-Villars. Paris, 1877.

[27] Rosseland S. Theoretical Astrophysics. Clarendon Press, Oxford, 1936.

[28] Bestman AR. The boundary-layer flow past a semi-infinite heated porous plate for two-component plasma. Astrophysics and Space Science 1990; 173: 93-100.